PNAS
www.pnas.org

Supplementary Information for

Kelp-forest dynamics controlled by substrate complexity

Zachary Randell, Michael Kenner, Joseph Tomoleoni, Julie Yee and Mark Novak

Corresponding Author: Zachary Randell
E-mail: randellzoregonstate.edu

This PDF file includes:

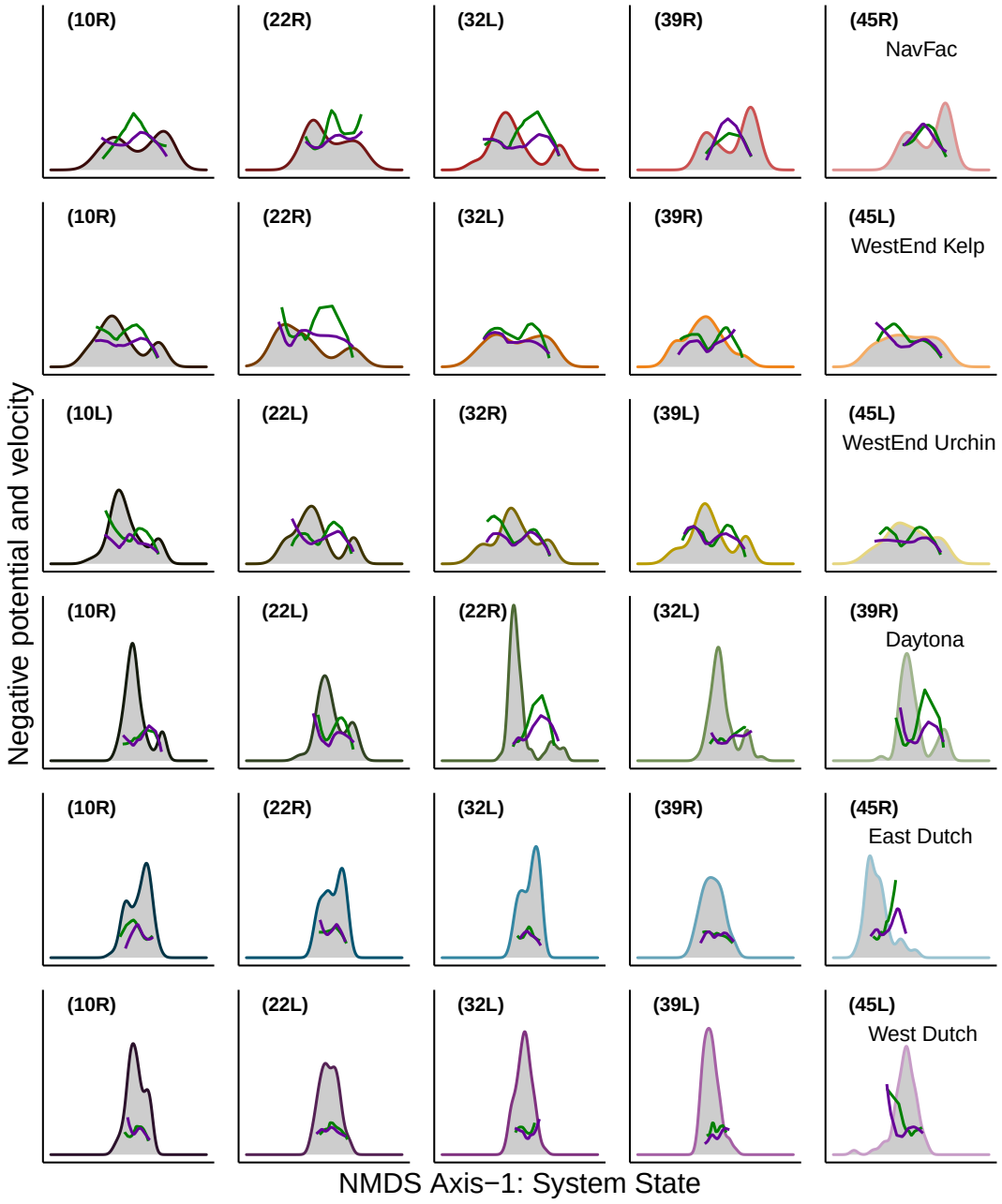

Fig. S1. Negative potential landscapes and directional velocities of community shift for all 30 transects evidence that movements towards the urchin-barren state (purple loess-smoothed lines) and towards the algal-only state (green loess-smoothed lines) exhibit low within-state velocities and high between-state velocities.

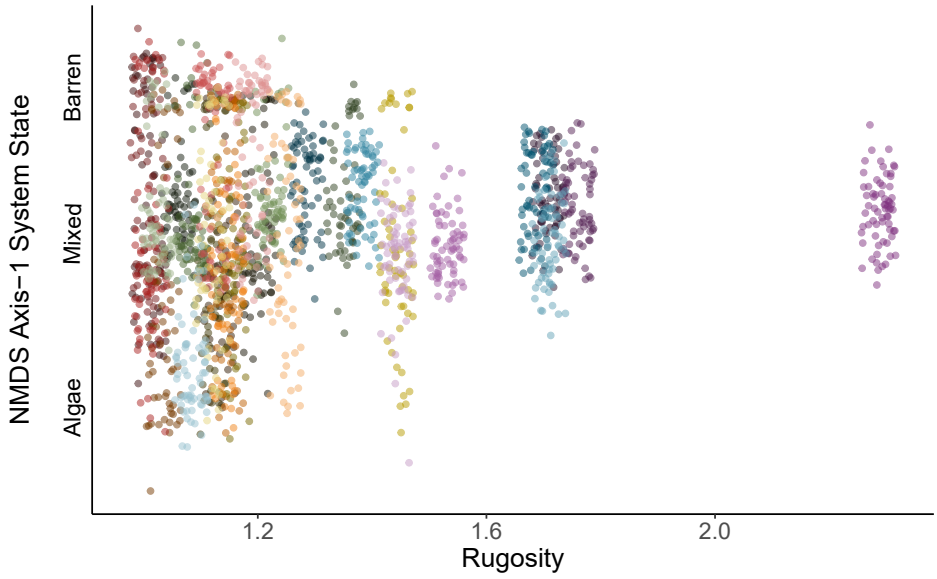

(a)

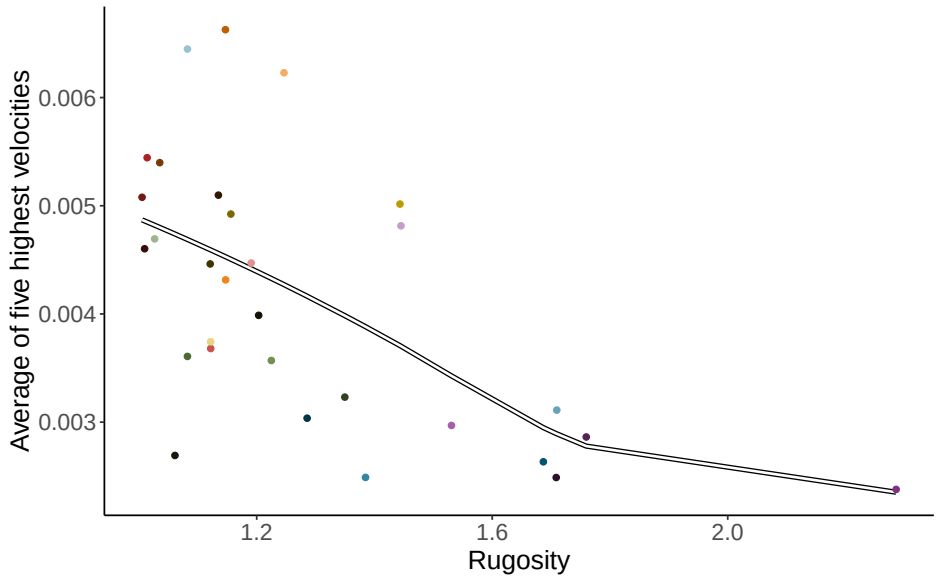

(b)

Fig. S2. (*a*) System state (*NMDS Axis-1 System State* from Fig. 2*a-f*) versus substrate rugosity. Points are jittered horizontally by 0.3 in *ggplot2* (1). (*b*) Points are the average of the five highest velocity movements per transect plotted against transect rugosity, demonstrating that the velocity of community shift decreases with increasing rugosity. The white line is loess-smoothed with a span of 1.

Table S1. Evidence for multi-modality as assessed using Gaussian mixture models fit to individual transects.

Site	Transect	n	Clusters	Mixing Probabilities	Means	Variances
NavFac	10R	65	3	0.49; 0.19; 0.30	-0.32; 0.46; 0.78	0.048; 0.02; 0.004
NavFac	22R	66	2	0.58; 0.41	-0.22; 0.54	0.035; 0.551
NavFac	32L	67	2	0.82; 0.17	-0.29; 0.81	0.08; 0.001
NavFac	39R	67	3	0.27; 0.19; 0.53	-0.22; 0.13; 0.72	0.003; 0.02; 0.005
NavFac	45R	67	2	0.48; 0.51	0.003; 0.70	0.047; 0.005
W.E. Kelp	10R	64	2	0.81; 0.18	-0.35; 0.62	0.08; 0.0005
W.E. Kelp	22R	64	2	0.78; 0.21	-0.65; 0.54	0.089; 0.014
W.E. Kelp	32L	64	3	0.53; 0.24; 0.21	-0.49; 0.23; 0.62	0.07; 0.01; 0.0003
W.E. Kelp	39R	64	1	1	-0.23	0.16
W.E. Kelp	45L	64	2	0.83; 0.16	-0.2; 0.64	0.17; 0.0004
W.E. Urchin	10L	64	2	0.57; 0.31; 0.10	-0.04; -0.22; 0.64	0.11; 0.009; 0.00008
W.E. Urchin	22L	64	2	0.81; 0.18	-0.37; 0.59	0.07; 0.003
W.E. Urchin	32R	64	2	0.9; 0.1	-0.18; 0.61	0.15; 0.0003
W.E. Urchin	39L	64	2	0.83; 0.16	-0.24; 0.63	0.108; 0.0008
W.E. Urchin	45L	64	2	0.83; 0.16	-0.17; 0.62	0.14; 0.0002
Daytona	10R	66	2	0.87; 0.13	0.08; 0.68	0.02; 0.001
Daytona	22L	58	2	0.79; 0.2	0.03; 0.59	0.03; 0.002
Daytona	22R	66	2	0.86; 0.13	-0.09; 0.71	0.01; 0.01
Daytona	32L	66	2	0.84; 0.15	0.05; 0.66	0.02; 0.01
Daytona	39L	60	3	0.13; 0.55; 0.30	-0.2; -0.04; 0.3	0.0001; 0.009; 0.14
East Dutch	10R	68	2	0.42; 0.57	-0.003; 0.37	0.02; 0.01
East Dutch	22R	68	4	0.27; 0.18; 0.07; 0.47	-0.1; 0.08; 0.19; 0.37	0.004; 0.0005; 0.00002; 0.004
East Dutch	32L	68	2	0.41; 0.58	0.018; 0.33	0.011; 0.0059
East Dutch	39R	68	1	1	-0.06	0.046
East Dutch	45R	68	2	0.87; 0.12	-0.7; -0.15	0.02; 0.02
West Dutch	10R	69	1	1	0.15	0.03
West Dutch	22L	69	1	1	0.1	0.03
West Dutch	32L	69	1	1	0.08	0.02
West Dutch	39L	69	1	1	-0.09	0.025
West Dutch	45L	69	2	0.10; 0.89	-0.54; -0.08	0.12; 0.02

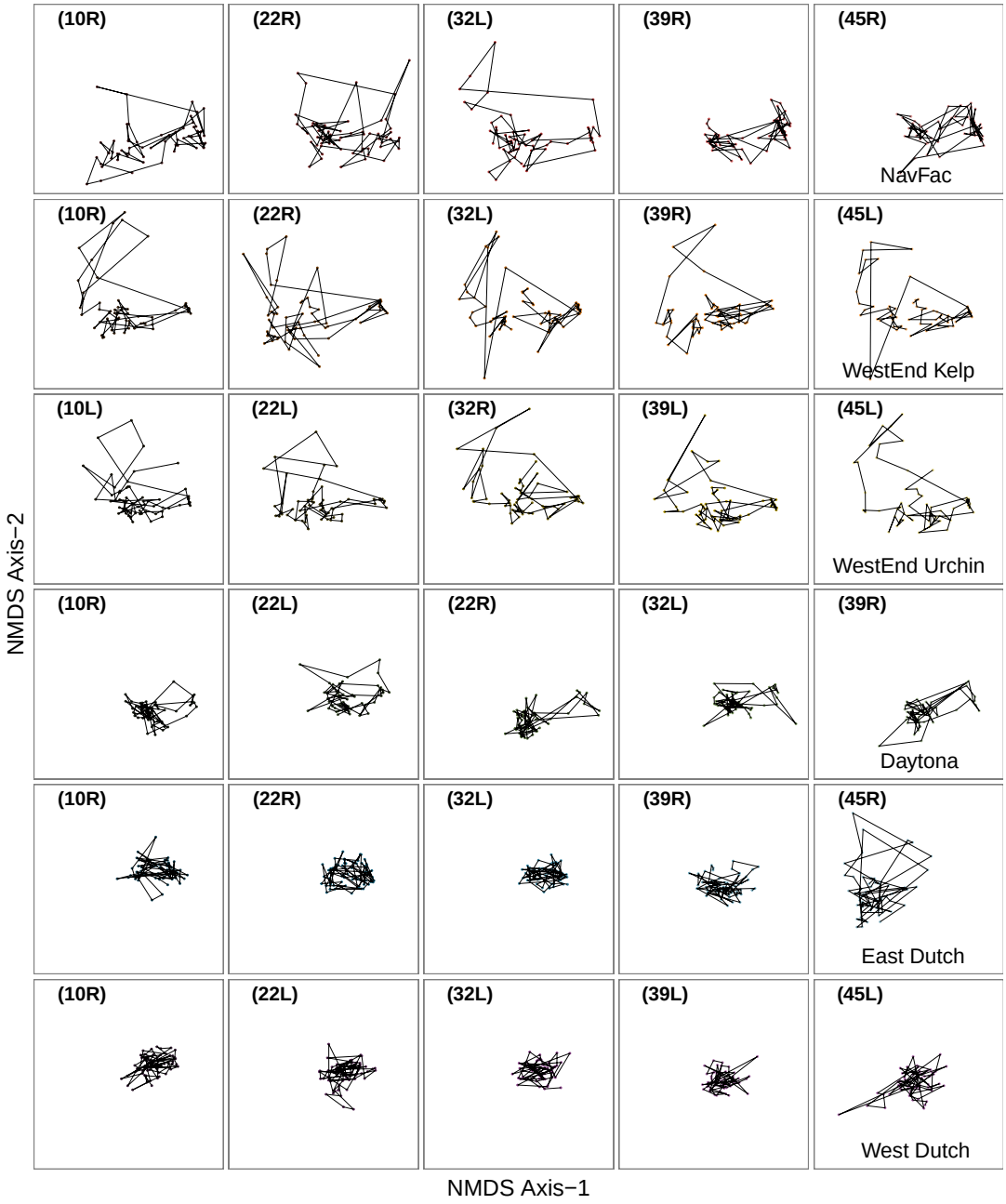

Fig. S3. Trajectories through two-dimensional species-space for all 30 transects. Substrate rugosity increases by row across sites. Note the extending periods of fluctuating community structure at both WestEnd sites which we interpret as long-term transients through an algal-only state, and that transects exhibiting high-velocity kelp fluctuations do not associate with substrate complexity along Axis-2.

Supporting Information Text

Environmental variables.

Overview. To assess whether potentially confounding environmental variables were associated with substrate complexity and kelp-forest dynamics, we analyzed 21 years of daily satellite-derived chlorophyll a data (2000-2021), 4 years of water temperature measurements (2015-2019), and 11 months of wave height measurements (2015-2016) taken at our sites and around San Nicolas Island. The chlorophyll a data were obtained from NASA's MODIS-Terra satellite (2) from which we considered measurements taken from within $3km$ buffers around our sites (Fig. S4a). (Because of their sub-$3km$ proximity, we combined Dutch Harbor and Daytona and subsequently refer to regions rather than sites for the chlorophyll a data). Temperature and wave height were measured *in situ* using sensors deployed at four sites—NavFac, WestEnd, Dutch Harbor, and Daytona—that encompass the entirety of kelp-forest dynamics we observed at SNI (Fig. S4a).

We visually assessed these data by plotting: (*1*) the time series for temperature and wave height; (*2*) kernel density plots for chlorophyll a, temperature, and wave height; and (*3*) inverse empirical cumulative distributions (eCDFs)—depicting the probability of observing measurements of equal or greater magnitude than a given magnitude—for chlorophyll, temperature, and wave height. We also used nonparametric two-sample Kolomogorov-Smirnov (KS) tests (3) to quantitatively compare the distributions of each variable among all pairs of regions/sites (Fig. S2).

Our inferences are summarized as follows (with additional context and details below): Chlorophyll a (Fig. S4b,c) and temperature (Fig. S5b,c) exhibited little to no biologically meaningful differences between sites. By contrast, NavFac and the two WestEnd sites located to the north and northwest of SNI experienced greater wave heights than did the sites located to the south and southeast of SNI. Large wave events are known to perturb kelp forests and thereby elicit shifts in state from kelp forests to urchin barrens (4). However, variation in wave height is a less parsimonious explanation than substrate complexity for the dynamics we observed around SNI because we also observed state shifts at the site with the lowest mean and maximum measured wave heights (i.e. Daytona).

Chlorophyll a. Concentrations of chlorophyll a can be indicative of the extent to which cold, nutrient rich waters reach the surface to promote not only planktonic but also benthic algal growth. We used $3km$ wide bands around sites ("regions") to investigate whether chlorophyll varied systematically among our sites. We were unable to reliably investigate site-specific differences due to the proximity of Daytona and the two Dutch Harbor sites (Fig. S4a) relative to the $1km$ grain size of the chlorophyll data. That said, the three measured regions encompass the oceanographic and bathymetric features around each site that could affect nutrient delivery.

Sea surface imagery was obtained by NASA's MODIS Terra satellite (2) and processed into chlorophyll a (mg/m^3). We analyzed *Level 2* data which are not aggregated spatially or temporally but instead contain daily observations, removing `NA`'s caused by cloud cover. Data were retrieved for each day between 24 February 2000 and 11 June 2021. We rarefied measurements across the regions by randomly subsampling measurements from the North ($n = 11,465$) and SouthEast ($n = 20,981$) regions to the sample size of the region with the lowest number of raster cells containing non-`NA` chlorophyll data (SouthWest $n = 10,262$).

Table S2. Results of two-way Kolmogorov-Smirnov tests applied to each pair of regions (for chlorophyll *a*) and sites (for temperature and wave height). The reported D statistic takes a value of 0 for identical distributions and a value of 1 for disparate distributions.

	Chlorophyll	Temperature	Wave Height
North & SouthWest	0.067	-	-
North & SouthEast	0.073	-	-
SouthWest & SouthEast	0.128	-	-
NavFac & EastDutch	-	0.110	0.128
NavFac & WestEnd	-	0.070	0.421
NavFac & Daytona	-	0.044	0.153
WestEnd & EastDutch	-	0.058	0.495
WestEnd & Daytona	-	0.043	0.530
Daytona & EastDutch	-	0.071	0.137

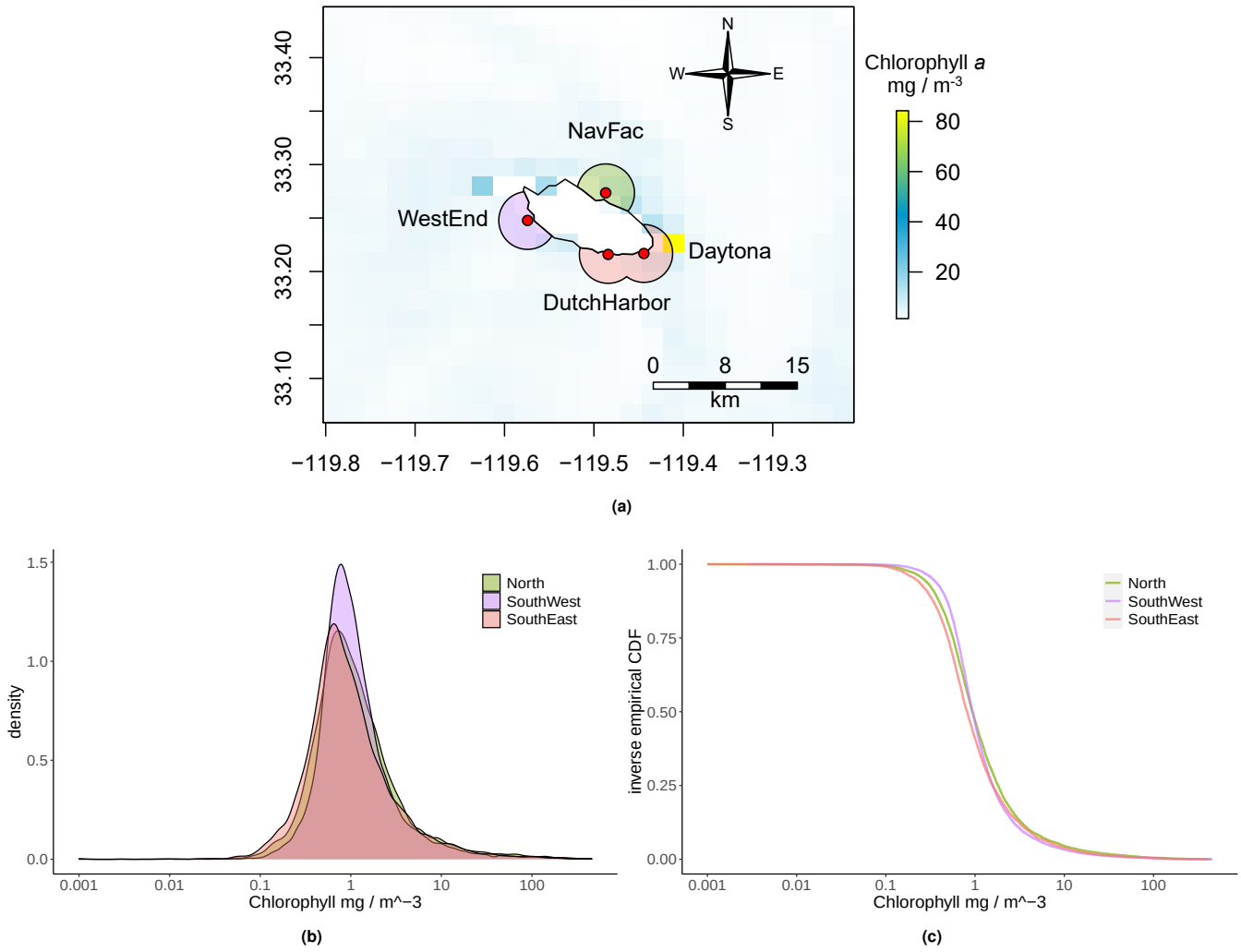

Fig. S4. (*a*) Chlorophyll *a* concentrations (mg/m^3) recorded 13 June 2020 overlain on a map of SNI with $3km$ buffer regions around the sites. The red dots indicate the locations where temperature and wave height sensors were deployed. (*b*) Kernal densities and (*c*) eCDFs of chlorophyll *a* concentrations by region.

Water Temperature. Four Hobo temperature sensors were deployed at 10-14m depth at four of the six sites (Fig. S4a), recording temperature once every hour. We restricted our analyses to the time-period when all four sensors were concurrently deployed, from November 11th 2015 to October 2nd 2019 ($n = 33,766$ observations per site; $n = 135,064$ total observations).

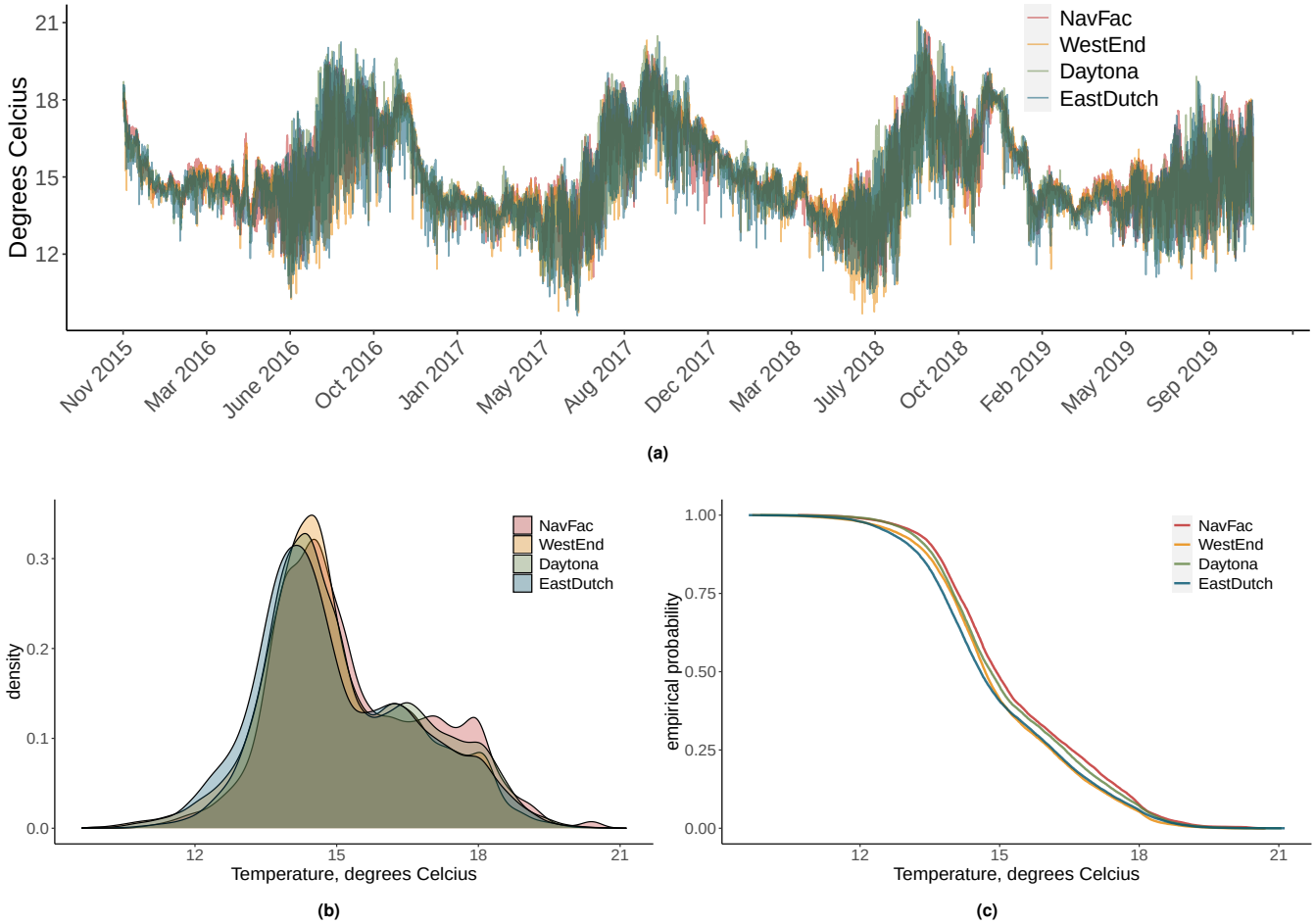

Fig. S5. (*a*) Time series (*b*) kernal densities, and (*c*) inverse eCDFs of hourly temperatures by site.

Wave height. A pressure sensor was deployed at each of the same four sites where temperature sensors were deployed (10-14m depth). Measurements were calibrated to estimate wave-height (in meters). We analyzed $n = 12,453$ sample points for each of the four sites from the period of 11 Nov 2015 - 25 Sep 2016 when all four sensors were deployed (5).

During this period, WestEnd and NavFac experienced pronounced large wave events that the other two sites do not (Fig. S6b). Further, WestEnd did not experience the same calm conditions experienced by the other sites (Fig. S6c). Nonetheless, in addition to observing shifts in community state at the high wave height sites (at the two WestEnd sites and at NavFac), we also observed community shifts at Daytona, the site that exhibited the lowest range of wave heights (Fig. S6c). We thus conclude that while large wave events are undoubtedly an important source of disturbance and a key proximate mechanism capable of eliciting shifts from kelp forests to urchin barrens, differences among sites in wave energy are not a more parsimonious (nor "upstream") explanation than substrate complexity for the dynamics we observed around SNI.

Additional urchin predators.

California sheephead. California sheephead (*Semicossyphus pulcher*) are capable of regulating urchin density and behavior (6–8). Sheephead were surveyed concurrent with the benthic surveys of the main text along five 50 x 4m benthic and midwater transects (9, 10). Their abundances were highest at the two high-complexity substrate sites, but were also high at Daytona, a low-complexity site (Fig. S7 & Fig. 2p, (9)). The high abundance of sheephead at Daytona was likely due to nearby high-complexity habitat with which they preferentially associate (8). The bimodality of Daytona's kelp-forest community states (Figs. 2d,j; 3d; S1 *row 4* & S3*row 4*) suggests that its sheephead abundances are insufficient to preclude shifts in community state, despite urchins being susceptible to predation along Daytona's relatively low-complexity substrate. Sheephead abundances alone are therefore not a more parsimonious (nor "upstream") explanation than substrate complexity for the dynamics we observed around SNI.

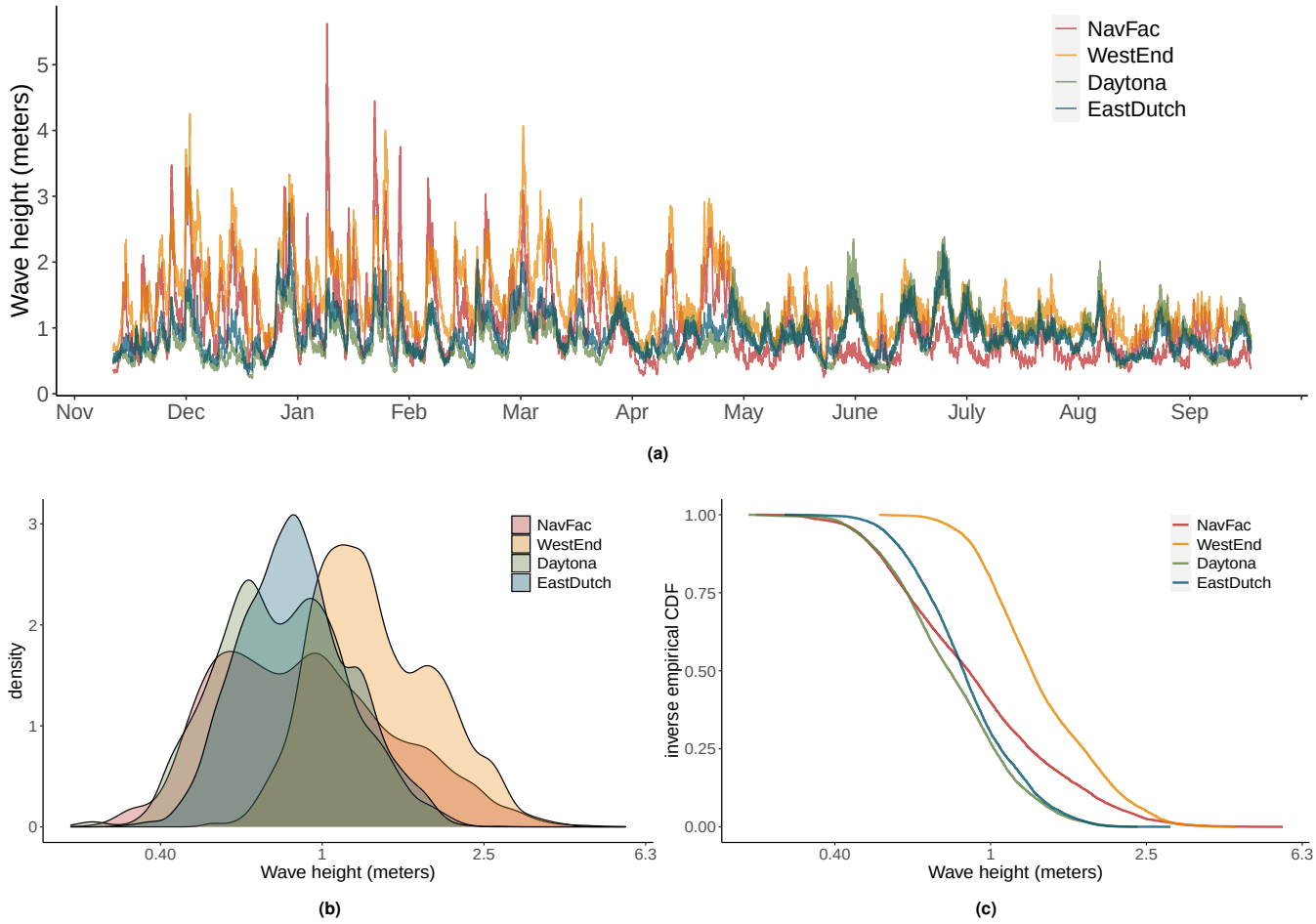

Fig. S6. (*a*) Time series, (*b*) kernal densities, and (*c*) inverse eCDFs of wave heights by site.

Sea otters. Southern sea otters (*Enhydra lutris nereis*) were reintroduced to SNI between August 1987 and July 1990 (11). The population hovered around 15 adult animals between 1990 – 1998 (11) and only exceeded 100 individuals for the first time in 2016 (12), with the great majority of individuals occupying the northwest end of the island until recently (11, 12). We infer that their population has been too low in abundance and their distribution around the island too spatially limited to influence the propensity for switching between kelp-forest states across our focal sites to date. Indeed, both shifts and persistent kelp-urchin coexistence were seen *prior* to sea otter translocation, and abrupt shifts continued after 1990, both in regions with and without consistent sea otter foraging activity. Nevertheless, we do not dismiss the possibility that sea otter predation contributed to the expression of the long-term transient algal-only state at the two West End sites (Fig. 3*b,c*), the formal evaluation of which is beyond the scope of this paper.

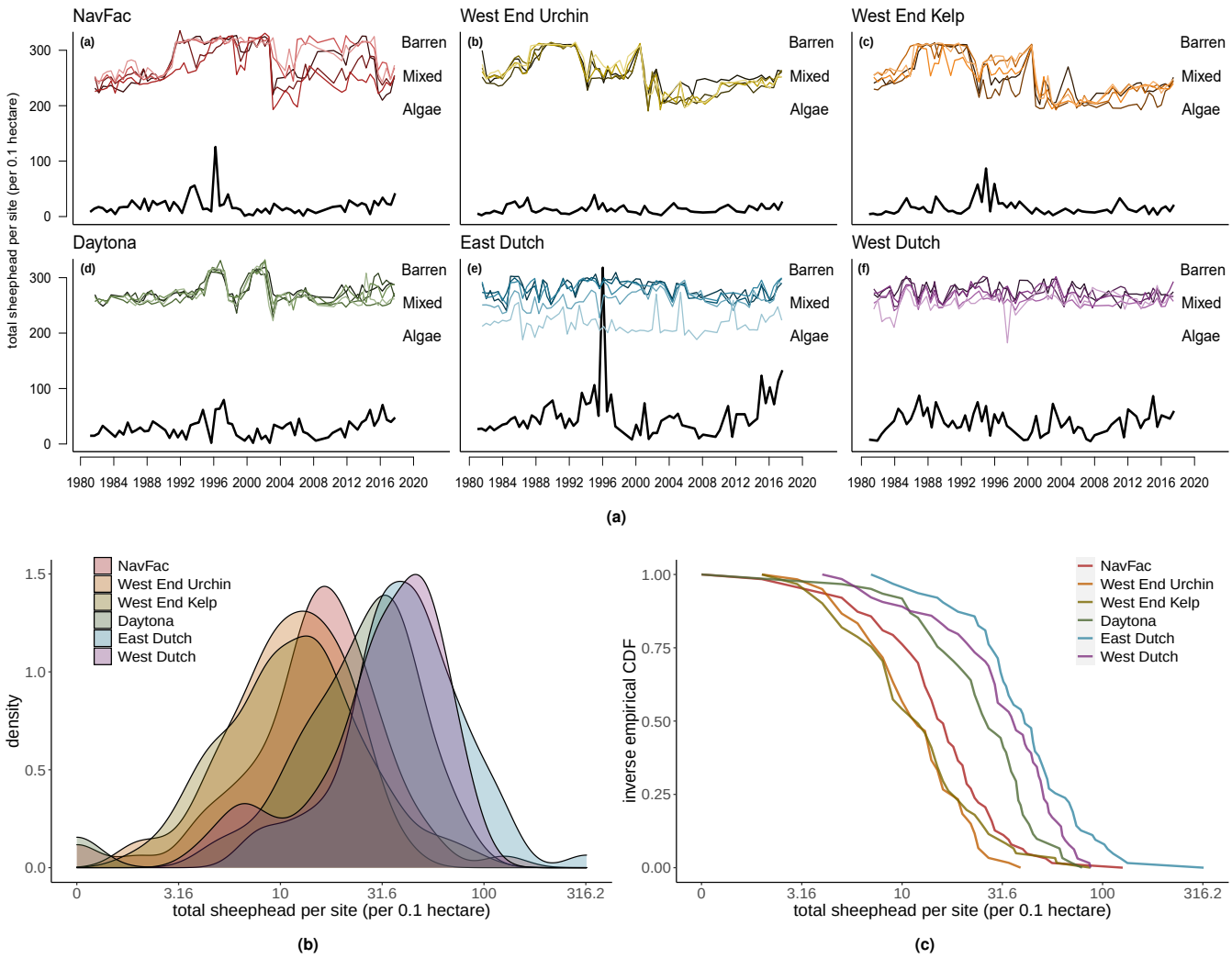

Fig. S7. (*a*) Site-total sheephead abundance visualized as time-series (black line, with the transect-specific dynamics of community state from Fig. 3: *NMDS Axis-1: System State* superimposed), and as (*b*) kernal densities, and (*c*) inverse eCDFs.

References

1. H Wickham, *ggplot2: Elegant Graphics for Data Analysis*. (Springer-Verlag New York), (2016).
2. OBPG NASA Goddard Space Flight Center, Ocean Ecology Laboratory, *Moderate-resolution Imaging Spectroradiometer (MODIS) Terra Ocean Color Data*, (2018 Reprocessing. NASA OB.DAAC, Greenbelt, MD, USA).
3. FJ Massey, The kolmogorov-smirnov test for goodness of fit. *J. Am. Stat. Assoc.* **46**, 68–78 (1951).
4. DC Reed, et al., Wave disturbance overwhelms top-down and bottom-up control of primary production in California kelp forests. *Ecology* **92**, 2108–2116 (2011).
5. K Lafferty, et al., *Hourly wave height and period hindcasts at 32 sites throughout the Channel Islands National Park and San Nicolas Island from 2000-2017: U.S. Geological Survey data release*, (2018).
6. SL Hamilton, JE Caselle, Exploitation and recovery of a sea urchin predator has implications for the resilience of southern california kelp forests. *Proc. Royal Soc. B: Biol. Sci.* **282**, 20141817 (2015).
7. JH Eisaguirre, et al., Trophic redundancy and predator size class structure drive differences in kelp forest ecosystem dynamics. *Ecology* **101**, 1–11 (2020).
8. RK Cowen, The effects of sheephead (Semicossyphus pulcher) predation on red sea urchin (Strongylocentrotus franciscanus) populations: an experimental analysis. *Oecologia* **58**, 249–255 (1983).
9. MC Kenner, et al., A multi-decade time series of kelp forest community structure at San Nicolas Island, California (USA). *Ecology* **94**, 2654–2654 (2013).
10. MC Kenner, MT Tinker, Stability and Change in Kelp Forest Habitats at San Nicolas Island. *West. North Am. Nat.* **78**, 633–643 (2018).
11. GB Rathbun, BB Hatfield, TG Murphey, Status of translocated sea otters at san nicolas island, california. *The Southwest. Nat.* **45**, 322–328 (2000).

12. JL Yee, et al., Southern (california) sea otter population status and trends at san nicolas island, 2017-2020, Technical report (2020).